Characterization of urea-modified Palabora vermiculite

Herminio F. Muiambo[a,1], Walter W. Focke[a,2], Maria Atanasova[a,b] and Aida Benhamida[c]

[a]Institute of Applied Materials, Department of Chemistry and Department of Chemical Engineering, University of Pretoria, Private Bag X20, Hatfield 0028, South Africa

[b]Council for Geoscience, 280 Pretoria Street, Pretoria 0184, South Africa

[c]Faculty of Technology, Laboratory of Advanced Polymer Materials, University Abderrahmane Mira, Bejaia 06000, Algeria

Abstract

Replacing the exchangeable interlayer ions in Palabora vermiculite with magnesium, aluminium or iron(III) ions does not affect the exfoliation onset temperature (456 ± 11 °C). However, co-intercalation of minor amounts of urea lowers the exfoliation onset temperature to 209 ± 35 °C. This significant decrease is attributed to the low thermal stability of urea which releases ammonia and water as blowing agents. Thermo-mechanical analysis indicates that the expanded vermiculite exhibits spring-like properties. Part of the original expansion is recovered when the applied force is removed. The observed hysteresis is attributed to the progressive flattening of warped/buckled sheets that make up the expanded worm-like structure. Provided the expanded flake has not been heated beyond 450 °C, it can be reconstituted by applying a sufficiently high compressive force followed by equilibration with distilled water. Such flakes show the conventional exfoliation behaviour when heated again.

Keywords: Vermiculite; urea; ion exchange; exfoliation; thermal mechanical analysis

---

[1] Permanent address: Department of Chemistry, Eduardo Mondlane University, P.O. Box 257, Maputo, Mozambique. E-mail address: hmuiambo@uem.mz.

[2] Corresponding author: Tel: +27 12 420 3728. Fax: +27 12 420 2516. E-mail addresses: walter.focke@up.ac.za, walter.focke@gmail.com (W.W. Focke).

1 INTRODUCTION

Vermiculite proper is a layered micaceous mineral formed by the hydrothermal alteration of mica (Brindley, 1980; Harben, 1990). Palabora vermiculite is not pure vermiculite but rather a mixed-layer vermiculite-biotite (Basset, 1961; Schoeman, 1989; Schwellnus, 1938). It is a product of the hydration of phlogopite/biotite mica exposed to percolating meteoric water under weathering conditions. During the vermiculization process there is progressive leaching of potassium alkali, an increase in the total water content, a change in colour and a simultaneous loss in elasticity and transparency on the part of the mica (Basset, 1961; Schoeman, 1989).

Palabora vermiculite shows considerable variability in its composition, cation exchange capacity (CEC) and ordering of the clay structure. This is attributed to differences in both the composition of the parent mica and the weathering conditions during its formation (Basset, 1961; Frank and Edmond, 2001). The hydrated interlayer cations (usually Mg^{2+}) of the vermiculite structure are exchangeable unlike the dehydrated K^+ cations in the biotite layers (Basset, 1961; Farmer and Wilson, 1970; Gast and Klobe, 1971; MacEwan et al., 1961; Newman and Brown, 1987; Schoeman, 1989).

When heated rapidly to elevated temperatures, vermiculite flakes expand in a vermicular, i.e., worm-like manner (Friedman et al., 1994; Wada, 1973b; Walker, 1961). The exfoliation of vermiculite can also be realized by the release of oxygen generated by the degradation of interlayer hydrogen peroxide (Groves, 1939). The expansion direction is perpendicular to the cleavage planes and modification occurs in a concertina-like fashion. The thermal expansion and partial splitting of the structure is due to sheet exfoliation forced by explosive release of interlayer water and its transformation into vapour (Baumeister and Hahn, 1976; Justo *et al.*, 1989; Obut and Girgin, 2002). It is conventional to call this expansion exfoliation even though the individual sheets that made up the original flake remain attached to each other. During the

2

exfoliation the bulk volume can increase by up to 30 times the original volume (Walker, 1961).

Vermiculite exfoliation occurs when the force generated by the inner vapour or gas pressure overcomes the ionic bonding forces between the layers (Hillier *et al.*, 2013). Thermo-mechanical analysis of neat and sodium-exchanged vermiculite revealed that the expansion behaviour varied considerably from flake to flake (Muiambo *et al.*, 2010).

Hillier *et al*. (2013) recently offered a plausible and convincing mechanism for the thermal exfoliation of vermiculite. They believe that intra-particle heterogeneities in the form of mosaic-like intergrowths of vermiculite, hydrobiotite and mica play a key role. A contiguous layer traversing a flake may be a vermiculite layer in one place and mica elsewhere. Furthermore, there may be internal boundaries where the nature of the vermiculite interlayer (with hydrated exchangeable cations) changes into a brucite-like interlayer hydroxide of chlorite. Both types of defect prevent complete sheet exfoliation and also act as internal physical barriers that prevent easy escape of the water vapour. The consequence is a build-up of internal pressure that generates forces that inevitably cause exfoliation when they exceed the interlayer bonding forces. The model explains why interstratified vermiculite has the greatest capacity for expansion; why smaller flakes expand less than larger ones as well as the asymmetry of the exfoliated vermiform particles.

Marcos *et al*. (Marcos et al., 2003) found that magnesium cations have a very strong affinity for water. Even under vacuum, the dehydration stops at the 1-WLHS state even at temperatures up to 120 °C. Our studies showed that the onset of explosive exfoliation coincides with reaching the one-water-layer-hydration state (1-WLHS). Furthermore, the event is associated with only a minor loss of water (Muiambo and Focke, 2012).

The degree of expansion depends on the flake size, the nature of interlayer cations, the presence or absence of interstratified phases, the heating rate and the terminal temperature (Huo *et al*., 2012; Justo *et al*., 1993; Marcos *et al*., 2009; Muiambo *et al*., 2010). For some

applications, e.g. intumescent fire barriers, lower exfoliation onset temperatures are desirable (Baumeister and Hahn, 1976; Langer and Marlor, 1981; Muiambo *et al.*, 2010; Wada, 1973a, b).

Urea is stabilized for agricultural purposes by intercalation into clays. This can be done by grinding and mixing of montmorillonite with molten urea (Abramova et al., 2007; Kim et al., 2011; Park et al., 2004). However, the low degradation temperature of urea and the preference of ligand water over urea in water metal complexes solutions may potentially pose problems (Park et al., 2004). Urea acts as a monodentate ligand for metal cations coordinating via the oxygen atom of the carbonyl group through ion-dipole interactions (Mortland, 1966; Orlova et al., 1985; Theophanides and Harvey, 1987). According to Mortland (1966) the urea bonding mechanism in clays depends on the nature of the interlayer cation. FTIR spectra indicate that the urea carbonyl oxygen in Fe-montmorrilonite and Al-montmorrilonite is protonated. This implies ion-dipole interactions between urea complexes and montmorillonite. In Mg-, Ca-, Li-, Na-, and K-montmorillonites, urea is bonded to the metal ion by coordination and possibly by ionization of the N-H bond. Abramova et al. (2007) found that some interlayer cations with low polarizing ability (e.g. K^+, Rb^+, Cs^+ and NH_4^+) are not suitable for the preparation of clay-urea complexes. Cations with high polarizing ability (e.g., Al^{3+} or Fe^{3+}) or transition metals (e.g., Co^{2+}, Ni^{2+} or Cu^{2+}) readily form urea coordination complexes even in the interlayer space of the clay. In the latter case, urea directly coordinates to the metal ion while in the former case the urea is protonated and linked to the interlayer cation via a water bridge. Brigatti et al. (2005) found only partial intercalation of urea-aluminium and urea-chromium complexes into vermiculite from water at 25 °C. Interestingly, attempts to prepare such complexes at 60 °C were unsuccessful.

On heating, urea and urea metal-complexes decompose and polymerize simultaneously releasing gaseous products (Schaber et al., 2004). The actual product spectrum depends on the

heating rate, final temperature and pressure, etc. (Brigatti et al., 2005; Chen and Isa, 1998; Orlova et al., 1985; Stradella and Argentero, 1993). The evolved gases contain ammonia, carbon dioxide and nitrogen oxides. Solid products include cyanuric acid, cyanic acid and biuret.

The present interest is to modify Palabora "vermiculite" so that it can provide a fire retardant effect in polymers similar to that achieved with expandable graphite (Krassowski et al., 2012). "The right place at the right time" flame retardant principle dictates that there should be a near perfect match between the exfoliation onset temperature of the expandable filler and the decomposition onset temperature of the host polymer. This means that the exfoliation onset temperature of ordinary commercial vermiculite is much too high for common polymers. It can be lowered by suitable chemical modifications under diverse conditions (Baumeister and Hahn, 1976; Langer and Marlor, 1981; Muiambo and Focke, 2012; Wada, 1973a, b). The present communication describes the tuning of the vermiculite's exfoliation onset temperature through intercalation of metal-urea complexes.

2. EXPERIMENTAL

2.1. Materials and methods

Mandoval Vermiculite supplied the micron grade (0.5 mm) sample of Palabora material. The CEC was 98 mEq/100 g (Muiambo et al., 2010). Flake thickness varied from about 30 μm to 300 μm. Urea and the metal chlorides of magnesium, iron and aluminium were sourced from Merck Chemicals, SA.

The temperature driven dynamic exfoliation process of the vermiculite was studied under a scanning electron microscope (FEI QUANTA 200 ESEM) fitted with a heating stage. The samples were placed inside a crucible and mounted in the heating stage. They were viewed at

5

200x magnification. The pressure was 0.5 kPa, voltage 20 kV, spot size 6-7 and a working distance of 16 – 20 mm. Temperature was ramped at 20 °C min^{-1}.

Samples (ca. 5 mg) were mixed with 100 mg dehydrated KBr and ground together with a mortar and pestle. The mixture was pressed into 13 mm in diameter discs. Fourier transform infrared spectroscopy (FTIR) spectra were recorded using a Perkin Elmer Spectrum RX FT-IR instrument. Reported spectra represent averages of 32 scans at resolution of 2 cm^{-1}.

Samples for chemical analysis were milled into fine powder (<75 µm). Carbon and sulphur content was determined on an Eltra CS 800 analyzer. The instrument was calibrated using the Euronorm-CRM 484-1 Whiteheart malleable iron, Euronorm-CRM 058-2 sulfur steel and Euronorm-CRM 086-1 carbon steel standards while instrument stability was monitored using the Council for Geoscience laboratory in-house reference standards. The detection limits for carbon and sulfur were of 0.017% and 0.009% respectively.

Chemical composition was determined with a PANalytical Axios X-ray fluorescence spectrometer (XRF) equipped with a 4 kW Rh tube. In this case the milled samples were roasted at 1000 °C for at least 3 hours to oxidize Fe^{2+} and S and to determine the loss on ignition (LOI).

Phase identification was carried out using X-ray diffraction (XRD). The PANalytical X-pert Pro powder diffractometer instrument featured variable divergence and receiving slits, and an X'celerator detector using Fe filtered CoKα radiation (λ = 0.17901 nm). The X'Pert High Score Plus software was used for data interpretation.

Thermogravimetric Analysis (TGA) was performed on a Mettler Toledo A851 TGA/SDTA instrument using the dynamic method. About 15 mg powdered sample was placed in open 150 µL alumina pans. Temperature was set from 25 to 1000 °C at a rate of 10 °C min^{-1} with air flowing at a rate of 50 mL min^{-1}.

Thermal expansion measurements were conducted on a TA instruments Q400 Thermo Mechanical Analyzer. The thickness of the tested flakes ranged from 81 µm to 431 µm. The flake expansion behaviour was measured with a flat-tipped standard expansion probe under a small preloaded force, e.g. 0.001 N. Individual flakes were sandwiched between the flat surface of the probe and the bottom surface of a 150 µl alumina pan. Temperature rate of 20 °C min^{-1} was used starting at ambient and going up to temperatures as high as 800 °C before allowed to cool down freely, typically to 50 °C. The expansion relative to the original flake thickness is reported. Various heating and cooling protocols in a nitrogen atmosphere, as well as varying the applied force, were explored. This included recompression of the expanded flake and soaking it in distilled water (added to the alumina pan) in attempts to rehydrate the flake over a period of 48 h.

2.2 Preparation of metal-urea vermiculites

Selected metal-urea complexes were prepared in a closed 500 mL vessel under constant agitation (200 rpm in an orbital shaker) for 2 h. The metal chloride to urea molar ratio was set at 1:6. vermiculite was added and the ion exchange reaction (between the cationic complex and the interlayer cation) was allowed to proceed for 15 days, based on the slow rate of exchange previously observed (Inoue, 1984; Kodama and Komarncni, 1999; Muiambo et al., 2010; Skipper et al., 1991). The complexes, in the reaction mixture, amounted to 150% CEC. The urea complex-modified vermiculites were rinsed with distilled water and allowed to air dry. The metal-exchanged vermiculites were prepared using the same procedure. All steps were executed at room temperature (Brigatti et al., 2005; Gast and Klobe, 1971).

3. RESULTS AND DISCUSSION

3.1. Mineralogical and chemical composition

Crude Palabora vermiculite used in this study has the following mineralogical composition (wt.%): interstratified mica/vermiculite (72), vermiculite (16), mica (6), dolomite (3) and apatite (3) (Muiambo et al., 2010).

The treatment with diverse salts and urea complexes did not visibly affect the macroscopic appearance of the material. The images in Fig. 1 show the appearance of Palabora vermiculite flakes before and after exfoliation at 800 °C. The ESEM micrograph in Fig. 2 shows an expanded flake exfoliated in the hot stage of the microscope. Closer inspection of individual flakes revealed numerous surface defects (striations, voids and folds) as well as edge damage. Granular impurities (not shown) were visible in between the flakes and on the surface of the aggregates. The latter might have been caused by milling of the material. Both Figures display the irregular growth of the concertina-like structure and the high variability in the gap size between the expanded sheets of the "worms". Careful study of video recordings of the expansion process conducted in the hot stage of the ESEM confirmed the heterogeneous nature of individual vermiculite flakes. Expansion occurred intermittently over a wide temperature range.
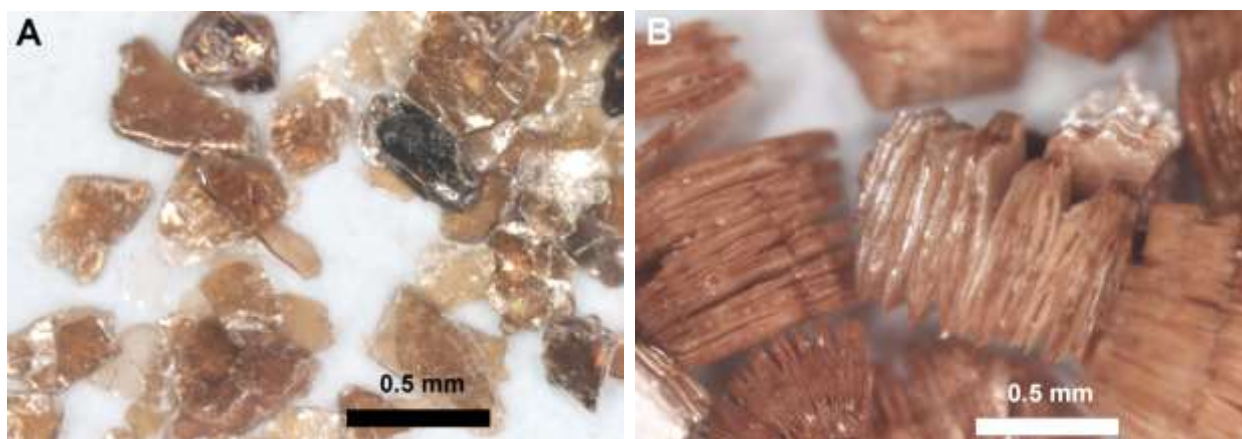
Fig. 1. Photographs of (A) neat Palabora vermiculite flakes, and (B) the expanded form after heating to 800 °C
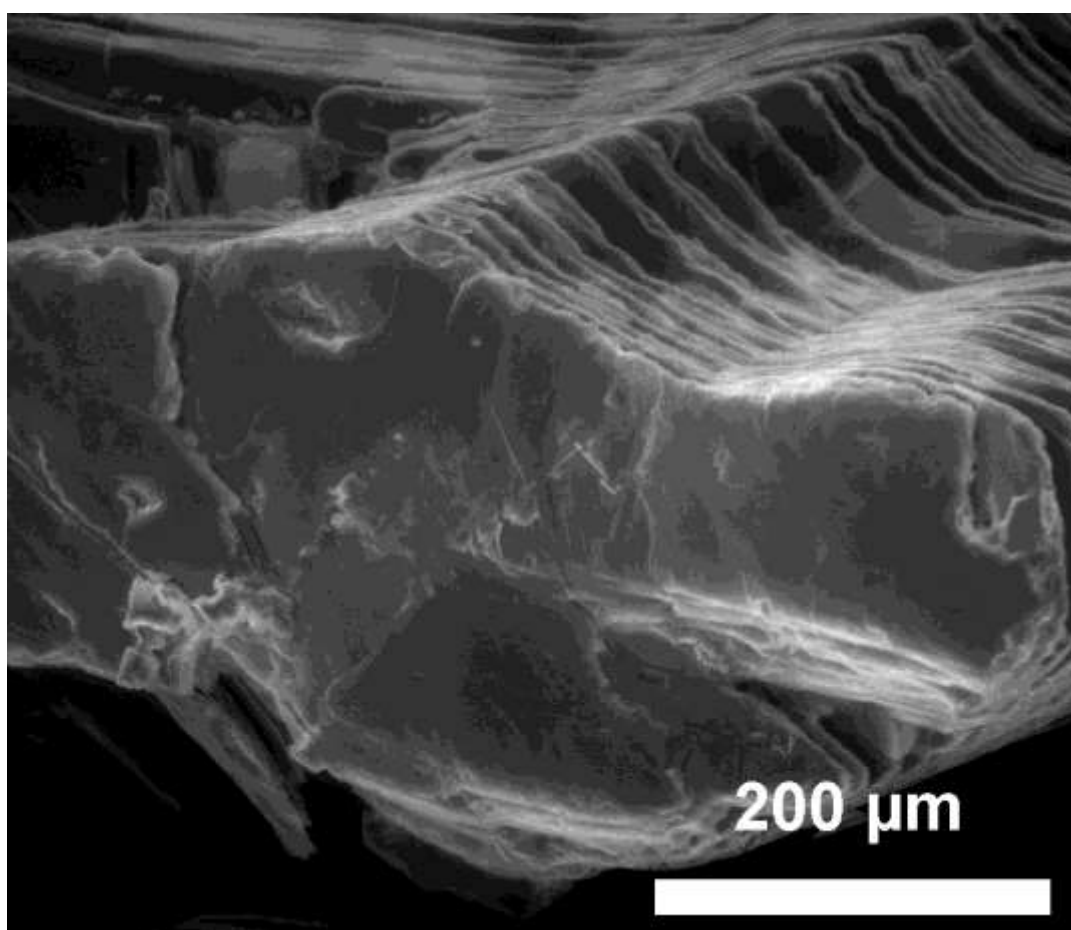

Fig. 2. ESEM image of a Palabora vermiculite flake exfoliated in the hot stage of the microscope.

The XRF results reported in Table 1 indicate that the potassium content was not materially affected by ion exchange with other metal cations or metal-urea complexes. This indicates that the K^+ cations present in the neat vermiculite were primarily associated with the biotite layers, i.e. they were non-exchangeable. Magnesium makes up the trioctahedral sheets and magnesium ions were the main interlayer cations in the neat material. Consequently the Mg^{2+} and magnesium-urea complex treated samples did not show a noteworthy increase in the magnesium content. However, a significant portion of the interlayer Ca^{2+} cations were substituted when Al^{3+}, Fe^{3+} and their respective urea complexes were intercalated. Nevertheless, a considerable amount of Ca^{2+} ions remained in the Mg-vermiculite and Mg-urea-vermiculite samples. This persistence probably stems from the unaffected dolomite $[CaMg(CO_3)_2]$ and apatite $[Ca_5(PO_4)_3(F,Cl,OH)]$ phases present in Palabora vermiculite.

Table 1. XRF composition analysis of neat vermiculite, metal exchanged forms and the corresponding metal-urea complexes.

Sample	Neat	Mg-urea	Mg	Al-urea	Al	Fe-urea	Fe
SiO_2	39.74	39.42	39.54	42.09	40.82	38.82	40.05
TiO_2	0.88	1.10	1.05	0.94	1.14	1.10	1.10
Al_2O_3	8.36	9.44	10.16	10.77	10.67	9.70	9.51
Fe_2O_3 (t)	7.06	9.60	8.12	8.29	9.98	10.48	11.03
MnO	0.05	0.06	0.06	0.05	0.06	0.06	0.06
MgO	22.70	21.87	24.21	22.56	22.14	21.30	21.25
CaO	5.72	3.90	3.42	1.56	1.37	1.84	2.96
Na_2O	0.01	0.26	<0.01	0.20	0.22	0.21	0.24
K_2O	4.81	4.74	5.07	4.17	4.37	4.37	4.32
P_2O_5	2.81	1.37	1.17	0.11	0.00	0.64	1.11
Cr_2O_3	0.02	0.06	0.03	0.05	0.06	0.05	0.05
LOI	7.83	7.15	7.02	7.72	7.96	10.29	7.18
Total	100.00	98.96	99.85	98.49	98.80	98.87	98.85

Table 2. Carbon and sulfur content of the neat and modified vermiculite forms.

Sample		Mg-urea	Al-urea	Fe-urea	Mg	Al	Fe
C	(wt.%)	0.45	0.32	0.65	0.04	0.04	0.04
S	(wt.%)	0.01	0.01	0.01	0.01	0.01	0.01
Urea[*]	(wt.%)	2.3	1.6	3.3	-	-	-
Urea[#]	(mmol)/100 g	37.5	26.4	54.5	-	-	-

[*]Estimated from the measured carbon content. [#]Since the CEC was 98 meq/100 g, the listed values also correspond closely to the percentages with respect to the CEC.
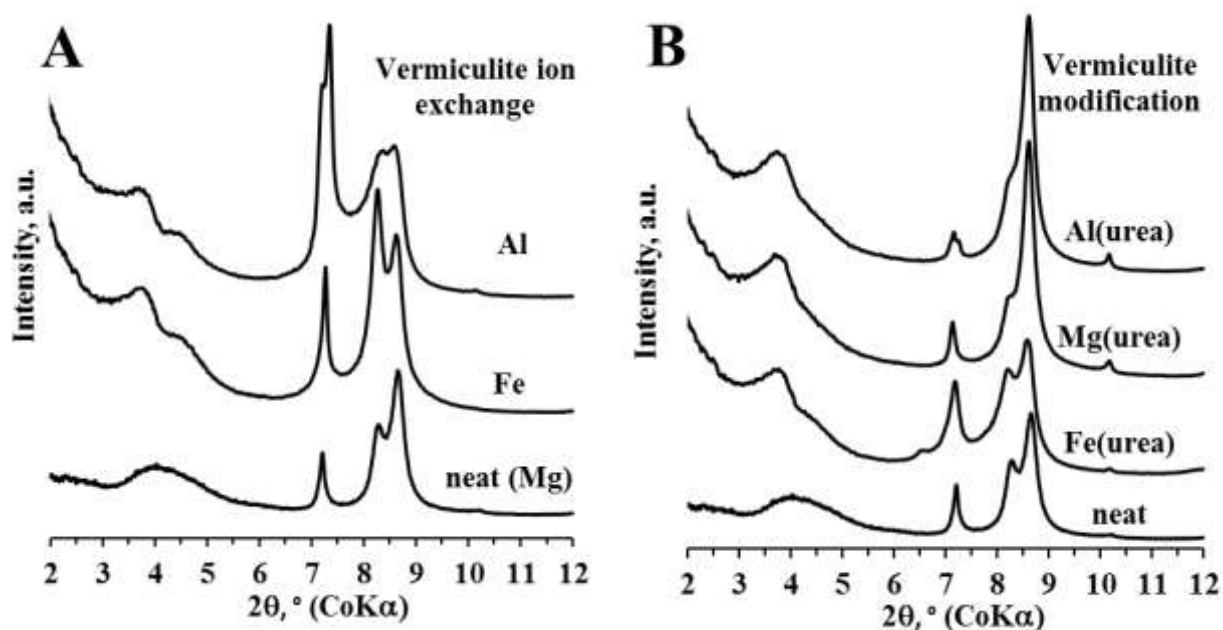
Fig. 3. X-ray diffractograms for neat Palabora vermiculite and its metal-exchanged forms and corresponding metal-urea complexes.

The carbon and sulphur elemental analysis results are reported in Table 2. As expected, there was no sulfur present while the carbon content increased with the intercalation of the urea complexes. Based on the vermiculite CEC (98 meq/100 g), the urea content corresponded to less than one urea molecule coordinated per metal ion present in the interlayer space. Low urea intercalation levels are also indicated for urea-modified montmorillonite clay studied by Abramova et al. (2007) and for samples that were subjected to washing (Park et al., 2004). The

11

interlayer urea/metal ratio was almost 0.6 for Fe-urea (60% CEC) while for Mg-urea and Al-urea it was about 0.3. The higher urea content found for Fe-urea is consistent with the higher loss on ignition (LOI).

Fig. 3 presents XRD diffractograms for crude Palabora vermiculite (in essence the magnesium form), its metal-exchanged forms and the corresponding metal-urea complexes. The crude material diffraction trace shows typical Palabora vermiculite features. The broad reflection at $2\theta = 4.03°$ (2.55 nm), the intense reflections at $2\theta = 8.28°$ (1.24 nm) and at $2\theta = 8.77°$ (1.19 nm) are indicative of the presence of interstratified phases. The reflection at $2\theta = 7.20°$ (1.43 nm) is consistent with the double-layer Mg-vermiculite phase. The weak reflection at $2\theta = 10.20°$ (1.01 nm) is from the mica (biotite or phlogopite) and it is present even after urea complexation (Mathieson, 1958; Newman and Brown, 1987; Pérez-Maqueda et al., 2003; Ruiz Amil et al., 1992).

In the metal-complexes (Fig. 3), the main reflection at $2\theta = 4.03°$ (2.55 nm) has shifted to lower 2θ values and increased in intensity. It has assumed the following values: $2\theta = 3.76°$ (2.72 nm), $2\theta = 3.70°$ (2.77 nm), $2\theta = 3.96°$ (2.59 nm), respectively to Fe^{3+}, Al^{3+} and Mg^{2+} complexes. In the Al^{3+} and Mg^{2+} complexes the reflection at $2\theta \approx 8.77°$ (1.19 nm) becomes more prominent at the expense of the reflection at $2\theta \approx 8.20°$ (1.25 nm).

3.2 Thermogravimetry analysis (TGA)

The thermogravimetric (TGA) curves for the unaltered material and the metal-exchanged forms are shown in Fig. 4 to Fig. 7. Mass loss commenced below 100 °C and occurred in several steps. The total mass loss recorded at 1000 °C was limited to 8-11 wt.% for all samples. Significant mass loss occurred in the first stage. This represents the loss of physisorbed (unbound) water and some of the water present in the galleries. The crude material showed a mass loss of 2.7 wt.% at 150 °C. Up to this temperature the vermiculites modified with Mg^{2+},

12

Al^{3+} and Fe^{3+} cations showed a greater mass loss than the crude material while for the corresponding urea complexes it was less. The same trend held for the total mass loss measured for the samples. The mass loss above 500 °C is attributed to dehydroxylation of the clay sheets. As will be shown below, all metal exchanged samples expanded in the temperature range 250 to 500 °C. On the other hand, the expansion happened between 200 and 250 °C for the urea-modified versions. Surprisingly, the observed mass loss in the temperature range where expansion occurred was relatively small, usually significantly less than 1 wt.%. The vermiculite modified by the urea complexes of Mg-, Al-, and Fe-urea showed mass losses of 0.4, 0.3 and 0.6 wt.% respectively. This may be compared to 0.2 wt.% for the crude material (Fig. 5). The expansion may be driven by the release of both water and volatile urea degradation products in this temperature range. Brigatti et al. (2005) studied aluminium-urea complexes intercalated in vermiculite. They reported the release of water and ammonia below 150 °C and CO_2 and HNCO at about 200 °C.
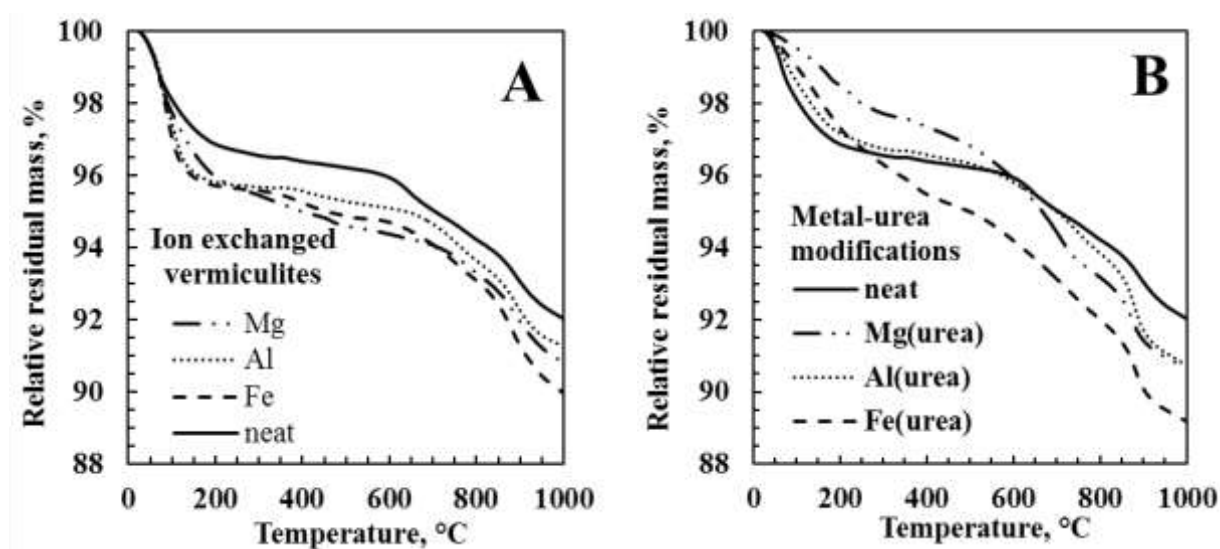

Fig. 4. Thermal behaviour of neat vermiculite and metal ion exchanged forms (A), and the corresponding metal-urea complexes (B).

13

3.3 Thermo-mechanical analysis (TMA)

Table 3, Fig. 6 to Fig. 10 summarise TMA results for neat vermiculite, its multivalent ion exchanged forms and the corresponding urea modified materials. Relevant plots showed that there is no correlation between flake size and expansion ratio. The data in Table 3 indicates that the maximum expansion ratio is also not affected by the type of modification. However, the expansion onset temperature does depend on the nature of the modification. Neat Palabora vermiculite expands abruptly at around 450 °C and contracts slightly on cooling (Muiambo et al., 2010). Previously we also found that exchanging the interlayer magnesium with sodium reduces the onset temperature by about 165 °C (Muiambo et al., 2010). The present urea-modified forms featured even lower average expansion onset temperatures (209 ± 35 °C).
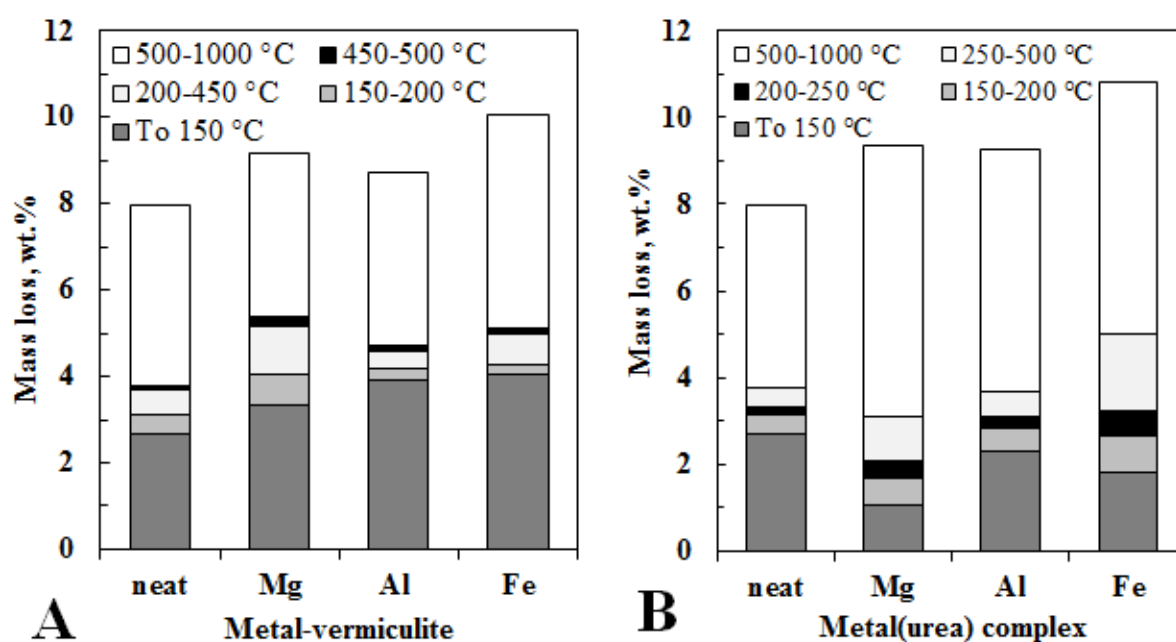

Fig. 5. TGA mass loss of (A) neat vermiculite, its metal-exchanged, and (B) the corresponding metal-urea complexes at selected temperature intervals. Most of the exfoliation occurred between 450 °C and 500 °C. The black bands correspond to the exfoliation temperature range.

14

Water is considered the exclusive blowing agent for the samples that did not contain urea (Hillier et al., 2013). Fig. 6 shows that ion exchange with Mg^{2+}, Al^{3+} or Fe^{3+} cations did not materially change the exfoliation onset temperature nor the maximum expansion ratio of the vermiculite. This was the case despite the fact that the water content had increased. This highlights the fact that not all the water released before the exfoliation plays a role in the exfoliation phenomenon. Similar results were found in our previous studies of vermiculite modified with ammonium-, alkaline- and alkaline earth metals (Muiambo and Focke, 2012). Abramova et al. (2007) previously studied the thermal decomposition of intercalated urea clay complexes. They found that the thermal degradation products are distinctly influenced by the nature of the interlayer cation. The lower expansion onset temperature of the urea-modified vermiculite is attributed to the low thermal stability of urea. Figure 10 shows an overlay of the TMA expansion curve for Mg-urea-vermiculite and the TGA mass loss curve for neat urea. Urea starts to decompose well below 200 °C releasing ammonia and water vapour that act as the blowing agents. The TMA curve suggests that the intercalated urea shows a slightly higher thermal stability. The exfoliation onset temperature of the urea modified forms (209 ± 35 °C) is within the intumescent systems activation temperature range (Morgan and Gilman, 2013) and future work will assess the utility of the urea-modified materials for this purpose.

15

Table 3. Summary of TMA results. The results pertain to single flakes using an applied force of 0.001 N. The flake thickness ranged from 30 μm to 467 μm with an average thickness of 174 μm.

| Expansion onset temperature, °C				
Vermiculite form	**Minimum**	**Maximum**	**Average**	**Std. Dev.**
Multivalent	440	467	456	11
Urea modified	174	290	209	35
Sodium exchanged	232	304	272	21
All samples	174	467	276	98
Maximum expansion ratio, -				
Vermiculite form	**Minimum**	**Maximum**	**Average**	**Std. Dev.**
Multivalent	5.3	8.6	7.1	1.3
Urea modified	5.0	14.7	8.3	3.0
Sodium exchanged	6.1	8.6	7.4	0.9
All samples	5.0	14.7	7.7	2.1
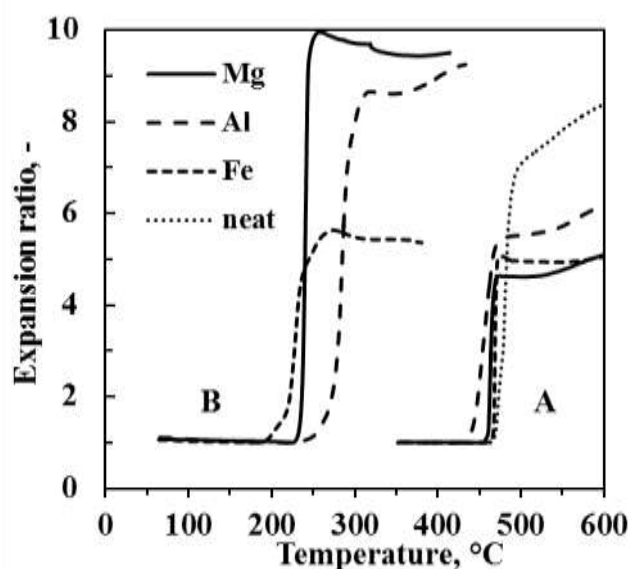
Fig. 6. Comparing the thermal expansion behaviours of (A) neat Palabora vermiculite and its multivalent ion exchanged versions with (B) the corresponding urea modified forms. Single flakes were heated up to 800 °C at 20 °C min^{-1} under an applied force of 0.001 N in nitrogen atmosphere.
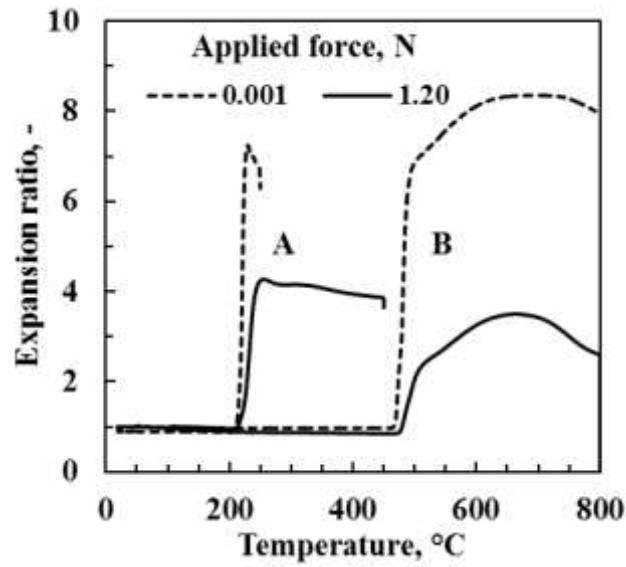
16

Fig. 7. Thermo-mechanical expansion of (A) Mg-urea modified vermiculite and (B) neat vermiculite as a function of the magnitude of the applied force.
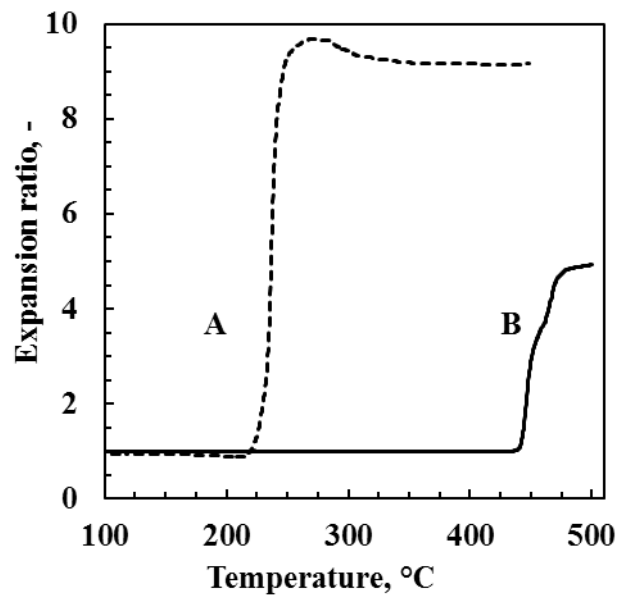

Fig. 8. Recovery of the capacity to expand. (A) Heating a single Mg-urea-modified vermiculite flake to 450 °C under an applied force of 0.001 N. (B) Re-heating the same rehydrated vermiculite flake to 500 °C after it was allowed to cool down, recompressed and soaked for 48 h in distilled water.
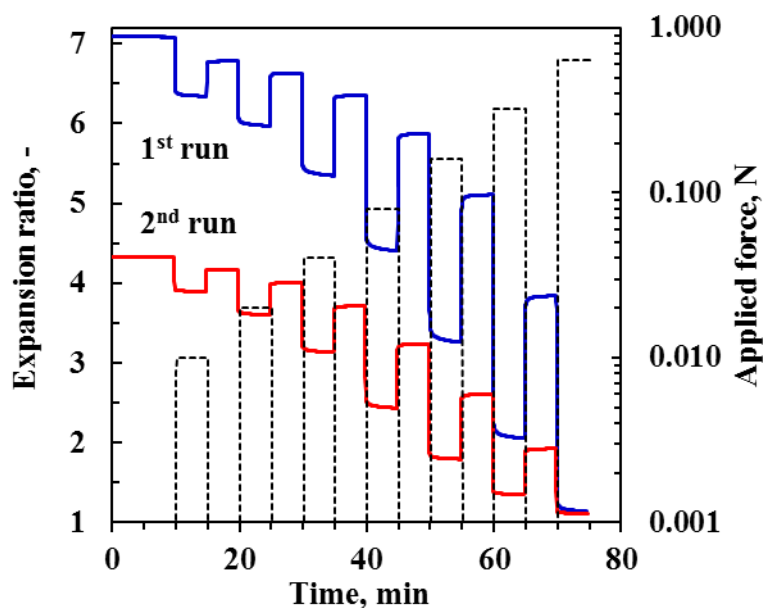
17

Fig. 9. The effect of varying the TMA applied forces on the compression of the same vermiculite flake described in Fig 8. The measurements were done at 50 °C. The applied force is indicated by the broken lines and it was doubled after each compression cycle.

Fig. 7 demonstrates the effect of the strength of applied force on the degree of expansion. While the expansion behaviour of individual flakes shows considerable scatter, indications are that flake expansion is reduced when higher forces are applied.

The results of an expansion, compression, rehydration and re-expansion experiment on an Mg-urea vermiculite sample are reported in Fig. 8 and Fig. 9. The experimental protocol was as follows: The sample was first heated to 450 °C and the expansion recorded. The flake was then allowed to cool down to 50 °C. The response to a cyclically applied force progressively increasing in strength was studied in the course of the experiment. Nearly full compression to the original thickness was achieved after applying the final load of 0.64 N. The compressed flake was then removed and soaked in distilled water for 48 h. It was then reloaded in the TMA and the experiment was repeated. The only difference was that the temperature was now scanned up to 500 °C.

18

Fig. 8 depicts the expansion behaviour as a function of the scanning time starting from the lowest temperature. As expected, the expansion curve exhibited the onset at around 215 °C, due to the release of urea and its volatile degradation products. After rehydration (48 h), the same flake showed thermo-mechanical behaviour similar to the neat or Mg-vermiculite, i.e. it displayed an expansion onset temperature to around 428 °C (2nd run) (Fig. 8). This illustrates the reversibility of vermiculite's expansion properties and also confirms that neat vermiculite's interlayer environment was successfully modified with urea molecules. Similar results were obtained with metal-vermiculite flakes except that the onset temperatures were similar.

Fig. 9 shows the effect of progressively applying stepwise increased force using the TMA followed by a reduction to a small force of 0.001 N. After each step there is an initial rapid decrease in the flake height followed by slower subsidence over time. When the force is reduced to a minimum the sample height recovers, though not completely. In addition a rapid recovery is followed by a slower increase in height. This implies that the expanded worm-like flake behaved like a spring that showed both hysteresis and slight creep behaviour.
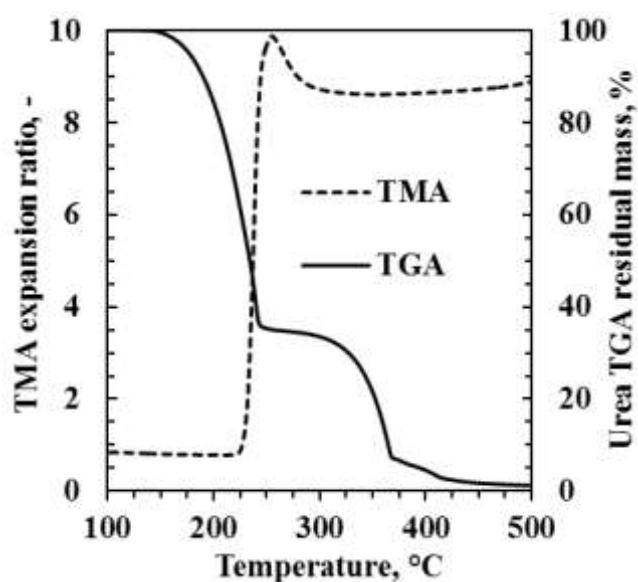

Fig. 10. TGA mass loss plot for pure urea and TMA expansion of Mg-urea vermiculite. Both samples were heated at 10 °C min^{-1} in a nitrogen atmosphere.

These observations conform well to- and can be interpreted in terms of the model postulated by Hillier et al. (2013). The expanded vermicular form comprises numerous partially delaminated sheets stacked on top of each other in an irregular manner. Probably the rapid expansion caused most, if not all, of these sheets to become mechanically deformed and distorted, i.e. bent, twisted, warped, buckled, etc. The mosaic-like defect patterns keep the whole structure together in a state of static equilibrium. However, when a sufficiently large mechanical force is applied the distorted sheets are flattened out and the original flake dimensions are approached. The original vermiculite structure is almost fully recovered when the compacted particle is equilibrated with water as it recovers the ability to expand again. When a smaller force is applied, only some of the warped sheets revert to the straightened state. The fraction flattened depends on the force that is applied. This explains the hysteresis observed in Figure 9: An expanded flake does not recover its fully expanded height once a force was applied. Furthermore, the extent of the recovery decreases as the compression force increases.

5. CONCLUSIONS

The expansion behaviour of Palabora vermiculite modified by ion exchange, in the presence or absence of urea, was studied. The maximum expansion ratio was independent of the flake thickness and the nature of the modification. Ion exchange with Mg^{2+}, Al^{3+} and Fe^{3+} did not materially affect the expansion onset temperature. However, co-intercalation of urea did reduce the expansion onset temperature significantly. This is attributed to the low thermal stability of the intercalated urea which decomposes and releases ammonia and water vapour as blowing agents.

Vermiculite samples expanded at temperatures up to 450 °C can be reconstituted into flakes that show the usual exfoliation behaviour. This requires application of a compressive force

sufficient to compact the vermicular structure back to the original dimensions followed by equilibration with liquid water.

At low compressive forces the vermicular structure shows spring-like behaviour (with hysteresis) that can be explained in terms of the vermiculite model postulated by Hillier et al. (2013). The expansion of vermiculite flake can be viewed as a bifurcation of potential equilibrium states. In the original particle the flakes are almost perfectly flat. In secondary expanded state the individual sheets comprising a flake assume a buckled configuration. Overall the structure is stabilized by a system of mechanical interconnects that prevent complete exfoliation/delamination. Ultimately it is the mosaic-like flaws present in the original particle (first observed by Hillier et al. (2013)) that provide the bonding that holds the sheets together. Individual sheets or, more likely neighbouring sets of sheets can snap back to the initial flattened and more stable state when subjected to a compressive force. Since the nature of the buckling varies among sheets, whether they do so will depend on the strength of applied compression force. This explains the fact that only part of the expansion is recovered when the compressive force is removed.

References

Abramova, E., Lapides, I., Yariv, S., 2007. Thermo-XRD investigation of monoionic montmorillonites mechanochemically treated with urea. Journal of Thermal Analysis and Calorimetry 90, 99-106.

Basset, W.A., 1961. The Geology of Vermiculite Occurrences. Clays and Clay Minerals 10, 61-69.

Baumeister, W., Hahn, M., 1976. An improved method for preparing single crystal specimen supports: H2O2 exfoliation of vermiculite. Micron 7, 247-251.

Brigatti, M.F., Laurora, A., Malferrari, D., Medici, L., Poppi, L., 2005. Adsorption of [Al(Urea)6]3+ and [Cr(Urea)6]3+ complexes in the vermiculite interlayer. Applied Clay Science 30, 21-32.

Brindley, G.W., Brown, G., 1980. Crystal structures of clay minerals and their X-ray identification. Mineralogical Society, London.

Chen, J.P., Isa, K., 1998. Thermal Decomposition of Urea and Urea Derivatives by Simultaneous TG/(DTA)/MS. Journal of the Mass Spectrometry Society of Japan 46, 299-303.

Farmer, V.C., Wilson, M.J., 1970. Experimental Conversion of Biotite to Hydrobiotite. Nature 226, 841-842.

Frank, D., Edmond, L., 2001. Feasibility for identifying mineralogical and geochemical tracers for vermiculite ore deposits. United States Environmental Protection Agency, Seattle, pp. 1-48.

Friedman, S.D., McKinney, R.W., Ou, C.C., Spotnitz, R.M., Wu, S., 1994. Vermiculite ore concentrate with specified specific density. Google Patents.

Gast, R.G., Klobe, W.D., 1971. Sodium-lithium exchange equilibria on vermiculite at 25 ° and 50 °C. Clays and Clay Minerals 19, 311-319.

Groves, R.C., 1939. Exfoliation of Vermiculite by Chemical Means. Nature 144, 554-554.

Harben, P.W., Bates, R. L., 1990. Industrial Minerals; Geology and world deposits. Industrial Minerals Division, Metal Bulletin Plc, London.

Hillier, S., Marwa, E.M.M., Rice, C.M., 2013. On the mechanism of exfoliation of 'Vermiculite'. Clay Minerals 48, 563-582.

Huo, X., Wu, L., Liao, L., Xia, Z., Wang, L., 2012. The effect of interlayer cations on the expansion of vermiculite. Powder Technology 224, 241-246.

Inoue, A., 1984. Thermodynamic study of Na-K-Ca exchange reactions in vermiculite. Clays & Clay Minerals 32, 311-319.

22

Justo, A., Maqueda, C., Perez-Rodríguez, J.L., Morillo, E., 1989. Expansibility of some vermiculites. Applied Clay Science 4, 509-519.

Justo, A., Pérez-Rodríguez, J.L., Sánchez-Soto, P.J., 1993. Thermal study of vermiculites and mica-vermiculite interstratifications. Journal of Thermal Analysis 40, 59-65.

Kim, K.S., Park, M., Lim, W.T., Komarneni, S., 2011. Massive intercalation of urea in montmorillonite. Soil Science Society of America Journal 75, 2361-2366.

Kodama, T., Komarncni, S., 1999. Alkali metal and alkaline earth metal ion exchange with Na-4-mica prepared by a new synthetic route from kaolinite. Journal of Materials Chemistry 9, 2475-2480.

Krassowski, D.W., Hutchings, D.A., Qureshi, S.P., 2012. Expandable Graphite Flake as an Additive for a New Flame Retardant Resin. GrafTech.

Langer, R.L., Marlor, A.J., 1981. Intumescent sheet material. Google Patents.

MacEwan, D.M.C., Ruiz-Amil, A., Brown, G., 1961. The X-ray identification and crystal structures of clay minerals. Mineralogical Society.

Marcos, C., Arango, Y.C., Rodriguez, I., 2009. X-ray diffraction studies of the thermal behaviour of commercial vermiculites. Applied Clay Science 42, 368-378.

Marcos, C., Argüelles, A., Ruiz-Conde, A., Sánchez-Soto, P.J., Blanco, J.A., 2003. Study of the dehydration process of vermiculites by applying a vacuum pressure: Formation of interstratified phases. Mineralogical Magazine 67, 1253-1268.

Mathieson, A.M., 1958. Mg-vermiculite: A refinement of the crystal structure of the 14.36 Å phase. American Mineralogist 43, 216-227.

Morgan, A.B., Gilman, J.W., 2013. An overview of flame retardancy of polymeric materials: Application, technology, and future directions. Fire and Materials 37, 259-279.

Mortland, M.M., 1966. Urea complexes with montmorillonite: an infrared absorption study. Clay Minerals 6, 143-156.

Muiambo, H.F., Focke, W.W., 2012. Ion exchanged vermiculites with lower expansion onset temperatures. Molecular Crystals and Liquid Crystals 555, 65-75.

Muiambo, H.F., Focke, W.W., Atanasova, M., der Westhuizen, I.V., Tiedt, L.R., 2010. Thermal properties of sodium-exchanged palabora vermiculite. Applied Clay Science 50, 51-57.

Newman, A.C.D., Brown, G., 1987. The chemical constitution of clays. Longman Scientific & Technical Mineralogical Society.

Obut, A., Girgin, I., 2002. Hydrogen peroxide exfoliation of vermiculite and phlogopite. Minerals Engineering 15, 683-687.

Orlova, V.T., Kudinov, I.B., Kosterina, V.I., Semendyaeva, N.K., Lepeshkov, I.N., 1985. Thermal stability of urea complexes of magnesium nitrate and magnesium monophosphate. Journal of Thermal Analysis 30, 1047-1051.

Park, M., Kim, C.Y., Lee, D.H., Choi, C.L., Choi, J., Lee, S.R., Choy, J.H., 2004. Intercalation of magnesium-urea complex into swelling clay. Journal of Physics and Chemistry of Solids 65, 409-412.

Pérez-Maqueda, L.A., Balek, V., Poyato, J., Pérez-Rodríquez, J.L., Šubrt, J., Bountsewa, I.M., Beckman, I.N., Málek, Z., 2003. Study of natural and ion exchanged vermiculite by emanation thermal analysis, TG, DTA and XRD. Journal of Thermal Analysis and Calorimetry 71, 715-726.

Ruiz Amil, A., Aragon de la Cruz, F., Vila, E., Ruiz Conde, A., 1992. Study of a material from Libby, Montana containing vermiculite and hydrobiotite; intercalation with aliphatic amines. Clay Minerals 27, 257-263.

Schaber, P.M., Colson, J., Higgins, S., Thielen, D., Anspach, B., Brauer, J., 2004. Thermal decomposition (pyrolysis) of urea in an open reaction vessel. Thermochimica Acta 424, 131-142.

Schoeman, J.J., 1989. Mica and vermiculite in South Africa. Journal of The South African Institute of Mining and Metallurgy 89, 1-12.

Schwellnus, C.M., 1938. Vermiculite Deposits in the Palaboroa Area, N.E. Transvaal. Government Printer, Pretoria.

Skipper, N.T., Soper, A.K., McConnell, J.D.C., 1991. The structure of interlayer water in vermiculite. The Journal of Chemical Physics 94, 5751-5760.

Stradella, L., Argentero, M., 1993. A study of the thermal decomposition of urea, of related compounds and thiourea using DSC and TG-EGA. Thermochimica Acta 219, 315-323.

Theophanides, T., Harvey, P.D., 1987. Structural and spectroscopic properties of metal-urea complexes. Coordination Chemistry Reviews 76, 237-264.

Wada, T., 1973a. Manufacture of expanded vermiculite employing a urea compound and low temperatures. Google Patents.

Wada, T., 1973b. Method for the expansion of vermiculite. Google Patents.

Walker, G.F., 1961. Vermiculite minerals, in: Brown, G. (Ed.), The X-ray identification and crystal structures of clay minerals. Mineralogical Society, London, pp. 297-342.